Hindawi
Advances in Materials Science and Engineering
Volume 2019, Article ID 6463576, 12 pages
https://doi.org/10.1155/2019/6463576

Research Article

Dynamic Behavior of Self-Piercing Riveted and Mechanical Clinched Joints of Dissimilar Materials: An Experimental Comparative Investigation

Yulong Ge and Yong Xia

State Key Laboratory of Automotive Safety and Energy, School of Vehicle and Mobility, Tsinghua University, Beijing 100084, China

Correspondence should be addressed to Yong Xia; xiayong@tsinghua.edu.cn

Received 28 June 2019; Revised 10 August 2019; Accepted 27 August 2019; Published 12 September 2019

Guest Editor: Rezwanul Haque

The present work compares the dynamic effect of a self-piercing riveted (SPR) joint with that of a mechanical clinched joint having the dissimilar materials combination. The substrates used in this investigation are aluminum alloy AA5182-O and deep drawing steel DX51D+Z. The static and dynamic behaviors and the failure modes of the SPR and clinching joints are characterized by lap-shear, cross-tension, and coach-peel tests. The influence of the strain-rate-dependent mechanical behavior of the substrates on the joints is examined; this can help improve prediction of the energy absorption of the joints under impact loading. Considering the realistic baking process in a painting shop, the deforming and hardening effects on the SPR and the clinched joints induced by baking are also studied. The specimens are heated to 180°C for 30 min in an oven and then cooled down in air. The SPR and the clinched joints before and after the baking process are compared in terms of the mechanical behavior.

1. Introduction

Currently, manufacturers of lightweight vehicles not only pursue more excellent structural performance of materials but also put effort into selecting or developing reliable technologies for joining dissimilar materials to achieve sufficient structural stiffness and crashworthiness. Among the combinations of dissimilar materials, joints with steels and aluminum alloys are the most prevalent ones applied to achieve viable and sustainable products. Mechanical, chemical, thermal, or hybrid joining processes can be selected to connect steel and aluminum alloy. The process could become complicated considering factors such as manufacturing conditions and cost. Self-piercing riveting (SPR) and mechanical clinching have many advantages and are quite suitable for manufacturing steel-aluminum joints. SPR demonstrates good mechanical and fatigue strength, while clinching has a lower manufacturing cost.

Suitable and cost-efficient mechanical joining technologies must be developed to utilize the weight reduction potential of steels combined with aluminum alloys and thus enable further affordable weight reduction in mass vehicle production. Mechanical joining technologies like SPR and mechanical clinching have been established in many automotive productions for joining multimaterial or light-metal car bodies, as these cold joining processes can be applied to joining dissimilar metals [1, 2].

SPR is used to join two or more sheets of materials by driving a rivet piercing through the top sheet or the top and middle sheets and partially piercing and locking into the bottom sheet to form a mechanical joint. During the SPR process, the spreading of the rivet skirt is guided by a suitable die, and the punched slug from the top sheet and the middle sheet is embedded into the rivet shank [3]. During the SPR process, the characteristic curve (force-displacement curve) can reveal the relationship between residual stress and its physical occurrence [4].

The mechanical clinching process is a method of joining sheet metal by localized cold forming of materials, which is also capable of connecting three layers of sheets [5]. The result

is an interlocking friction joint between two and more layers of material formed by a punch into a special die [6]. The die radius, depth, and die groove shape can affect the joinability, and the die groove width is the most important parameter affecting the material flow effect of the clinching process [7]. The analysis of clinched joints of DX51 and DP600 steels shows that increasing the joint diameter and forming force results in increased strength [8, 9]. In addition to round clinching, joints of square clinching tools are also used with orientation angles of 0° or 90° relative to the shearing load [10].

Comparing the production costs of these joining processes, clinching shows a lower running cost in the automotive industry. However, the mechanical characteristics of the joints are very different [11]. SPR joints have superior static and fatigue properties, while clinched joints also present favorable fatigue performance [12]. Higher strength is always observed in lap-shear testing compared with cross-tension testing [13]. As part of structural crashworthiness, dynamic tests are needed to study the dynamic behaviors of joints. Dynamic joint strength evaluation procedures have been introduced, and the dynamic strength data for SPR joints of dissimilar metals have been measured. It has been reported that the high speeds during dynamic tests can increase the joint strength and decrease the dissipated energy of steel-aluminum steels [14]. In addition, an experimental study on the behavior of SPR joints between aluminum AlMg3.5Mn and AlMg3.0Mn materials under dynamic loading conditions using a split Hopkinson tension bar in both the shearing and pulling-out direction was performed, showing a negligible rate effect on the joint [15]. Various failure modes may be observed in SPR joints. The three primary ones are rivet head pullout, rivet tail pullout, and sheet tearing [16]. Conversely, although there are insufficient studies on the dynamic behavior of clinched joints, they show a comparable energy absorption on the aluminum single-hat structure impact condition to the spot-welded joint with a suitable clinching process [17].

In this study, an aluminum alloy AA5182-O and mild steel DX51D+Z material combination is used. Exemplary results from lap-shear, cross-tension, and coach-peeling tensile tests are shown. The static and dynamic behaviors and the failure modes of both joints are characterized. In addition, as an increase in temperature can lead to a reduction in the strength of aluminum-magnesium alloys such as AA5182 [18], baked specimens are tested and compared to nonbaked ones in terms of their mechanical behavior to study the baking effect.

2. Experimental Procedure

Aluminum alloy AA5182-O and mild steel DX51D+Z are conventionally used for automobile body panels. The mechanical properties of the aluminum alloy and steel sheets are given in Table 1. The isotropic hardening law can be expressed using Swift's law:

$$\sigma = K \times \left(\varepsilon_0 + \varepsilon_p\right)^n, \quad (1)$$

Table 1: Mechanical properties of AA5182-O and DX51.

	AA5182-O	DX51D+Z
E (MPa)	6800	207000
υ	0.34	0.3
$\sigma_{0.2}$ (MPa)	90.7	165.4
K	506.9	473.2
ε_0	0.004	0.0055
n	0.302	0.229

where σ is the stress and ε_p is the plastic strain. K, ε_0, and n are material constants. The thicknesses of AA5182-O and DX51 were 0.85 mm and 1.20 mm, respectively, in this study.

The cross-sectional shapes of the joints are shown in Figure 1. The quality of an SPR joint from the cross-sectional perspective is primarily characterized in terms of the amount of mechanical interlock, known as rivet flaring, which is in the range of 300~400 μm in this case. The clinched joint is characterized by the following parameters [7]: the axial thickness of the sheets (707 μm), the thinning of the upper sheet (576 μm), and the clinch lock (121 μm).

Lap-shear, cross-tension, and coach-peel test specimens used to determine static strength are illustrated in Figure 2. In the lap-shear test, shear force is the main load induced on the joint, and the deformation behavior is limited to intrinsic deformation of the joint. Cross-tension specimens are used for normal direction tests. In addition, coach-peel tests were performed. DX51 is on the top, and AA5182-O is on the bottom.

AA5182-O material sheets for automotive BIW applications show softening behavior with respect to the prestrained sheets after the paint bake cycle. The specimens were placed in an oven at 180°C for 30 min and tested under static conditions to determine the influence of the baking process on the mechanical behavior of the joints.

A universal testing machine (Zwick Z020) and hydraulic testing machine (Zwick H5020) were used to conduct the static and dynamic tests, respectively. The global loading speeds were 0.083×10^{-3} m/s, 0.1 m/s, and 2 m/s. The digital image correlation method (VIC-2D) was adopted for deformation measurement. The gauge length of lap-shear and coach-peel specimens was 50 mm, and the displacements measured in cross-tension tests were the separative displacement of the fixtures, which are regarded as rigid.

The substrate materials have different responses to the strain rate effect. Previous studies have reported that a negative strain rate dependence of the material strength has been observed for Al-Mg alloys at a quasistatic strain rate, but there is a positive strain rate dependence for a high strain rate [19]. The yielding strain rate of DX51D+Z could increase by approximately 50% from static to intermediate strain rates [20].

Tests for lap-shear and coach-peel specimens under loading speeds of 0.1 m/s and 2 m/s were also performed to understand the mechanical behavior and failure modes of joints using a hydraulic high-speed testing machine. All tests were repeated three times to guarantee reproducibility, and the median result is shown.

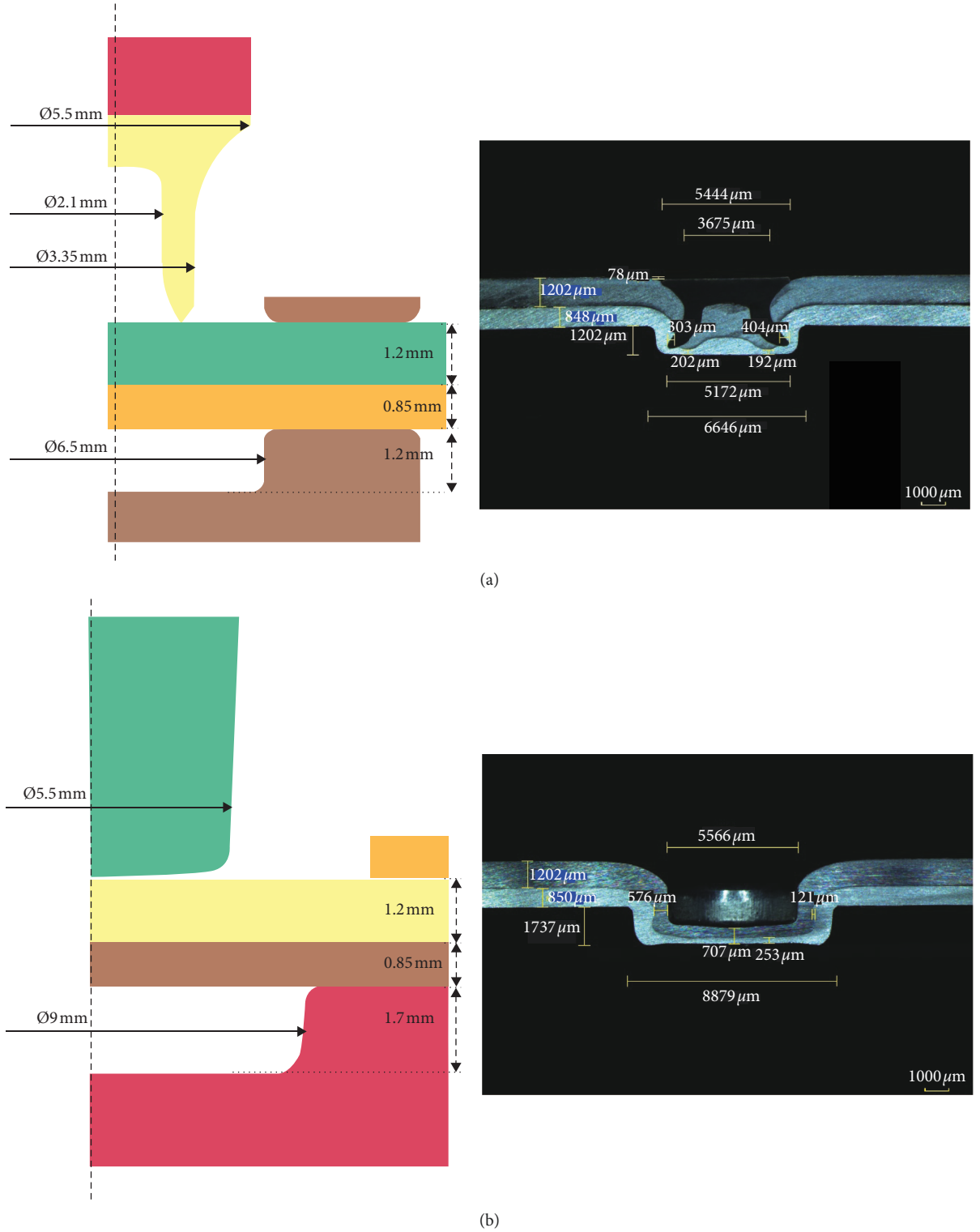

Figure 1: Tool geometries and cross-sectional shapes of (a) self-piercing joint and (b) mechanical clinched joint.

3. Results of Static and Dynamic Tests

3.1. Static Test. The force-displacement curves and failures for static lap-shear tests of joints obtained by both joining processes are illustrated in Figure 3. The maximum loads and stiffnesses, which are the slope of the linear stage, for the SPR joint and the clinched joint are similar. The elongation, however, is quite different. The deformation process of the SPR joint can be divided into three phases: elastic deformation, failure initiation, and failure extension. The rivet helps to prevent the steel sheet from being pulled out. As an alternative, the rivet moves in the aluminum sheet, which

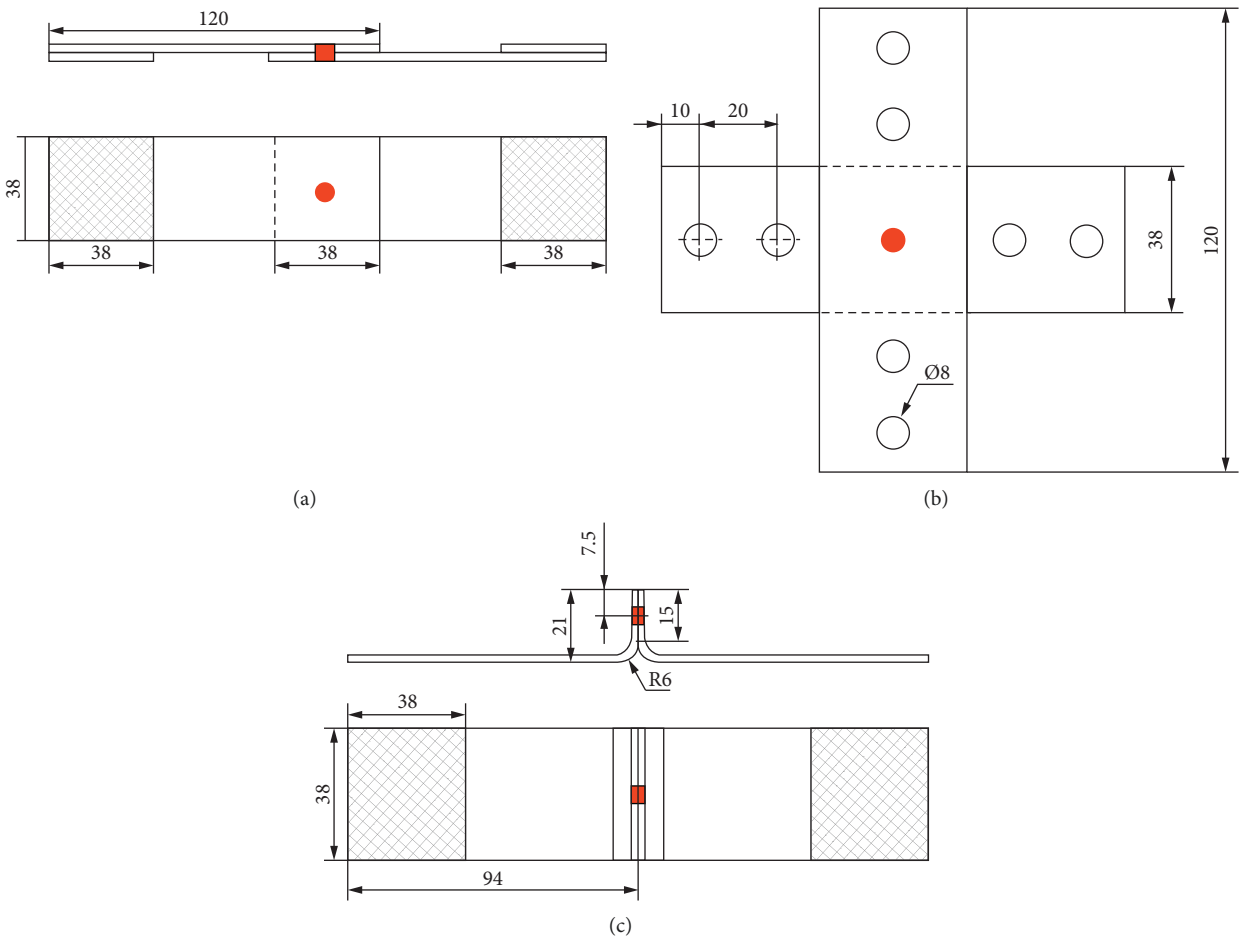

Figure 2: Specimens of joints for testing: (a) lap-shear, (b) cross-tension, and (c) coach-peel.

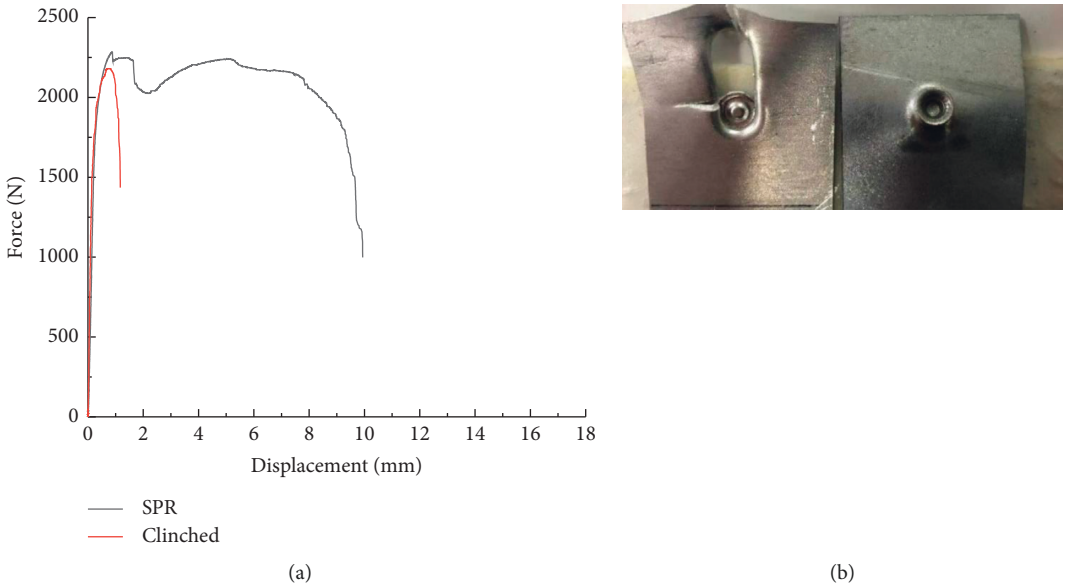

Figure 3: Continued.

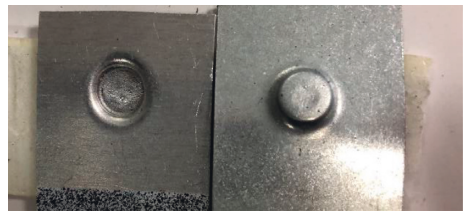

(c)

Figure 3: Static lap shear tests: (a) force-displacement curves, (b) material fracture failure mode of the SPR joint, and (c) pulling-out failure mode of the clinched joint at 0.083×10^{-3} m/s.

tears it apart and leads to a plateau in load before total failure. For the clinched joint, deformation breaks the geometry of the interlock, so that the load decreases rapidly. They have similar peak force-bearing capabilities, but the total energy dissipated of a single SPR joint is 10 times that of a clinched joint.

In these tests, as the strength of steel sheet is higher than that of the aluminum one, steel sheets on the top are bent up and large local deformation occurs on the button of the aluminum sheets, which results in joint failure. In the SPR joint, fracture can be found on the aluminum sheet from the button to the edge, bottom sheet tearing mode, which is not a common failure type in similar materials' joints. On the contrary, no large deformation occurs out of the button area in the clinched joint. The steel sheet is pulled out from the interlock on the aluminum sheet, and there is no material fracture on either sheet.

The force-displacement curves and failures for static cross-tension tests of the joints are illustrated in Figure 4. Unlike the lap-shear tests, the elongation and maximum loads are distinct, although the stiffnesses of the two joints are similar. The clinched joint has approximately 60% of the ultimate strength and of the SPR joint.

In terms of failure, pull-out is the dominant mode in both joints. Severe local doming occurs on the steel and aluminum sheets, and the strength of the steel sheets and rivets is higher, which leads to the expansion of clinched region on the bottom sheet. The interlocks in both joints are unbuttoned, so the steel sheets/rivets are plugged out, and no obvious material damage is found in either joint.

Similar mechanical behaviors are also observed in the static coach-peel tests, as the joints in these two forms primarily undergo a normal direction force, as shown in Figure 5. The deformation process of these aluminum-steel joints is more complicated. As the aluminum sheet of DX51 is stronger and thicker, when it is flattened by the moment, the bottom sheet of AA5182-O is rolled up in the joining regions, rather than flattened. This leads to sliding out of the interlocks of SPR and clinched joints and a pull-out failure mode. On the other hand, comparing the curves of two joints, the imbedded rivet tail can help to prevent the rivet from peeled out. Hence, a plateau in loading arises in the SPR joint before failure and the clinched joint fails right after peak loading.

From these tests, it can be seen that in the AA5182-O and DX51 joints under static conditions, the stiffness of the two joints is similar, but the toughness of the SPR joint is remarkably higher than that of the clinched joint. The normal strengths of these joints are much lower than their shear strengths. It is worth mentioning that plateaus appear when the loading reaches the peak of SPR joints under lap-shear and coach-peel conditions. This indicates that when the button begins to separate, the rivet can still help to bear the loading, but the clinched joint fails rapidly. Tail pull-out is the main failure mode in the cross-tension and coach-peel tests, which implies that it is better to prevent the joints from being exposed to a normal direction load.

3.2. Dynamic Test. Dynamic tests were conducted under global loading speeds of 0.1 and 2 m/s. Figure 6 shows the force-displacement curves and failure modes of the SPR joint at the two speeds and comparison to the quasi-static one. The stiffness and maximum strength of the joint are not significantly influenced by dynamic effects. Conversely, the ductility decreases from the 0.083×10^{-3} m/s condition to the 0.1 m/s condition and then remains at a similar value when the speed is increased to 2 m/s. The loading plateau disappears under dynamic conditions, so that a trapezoidal mechanical response degenerates to a triangular response. The total energy absorption capability decreases by more than 50%, from approximately 21 to 10 J.

Although the bottom sheet tearing is observed as the dominate failure mode, the modification of the curves could be the result of different dynamic behaviors with respect to the substrate materials. Generally, steels are more sensitive to strain rate effects than aluminum alloys, which contributes to the loss of load-bearing capability of the rivet tail. This leads to a transition of the deformation patterns on steel and aluminum sheets. At 0.083×10^{-3} m/s, the aluminum sheet remains flat during the tensioning process, and the steel sheet is bent. Conversely, as the yielding stress increases because of the strain rate effect, the steel sheet remains flat, while the aluminum sheet is bent, after which material failure occurs. The bent bottom sheets under dynamic conditions lead to a larger loading angle like peeling and a rapid failure.

Considering the coach-peel tests, Figure 7 demonstrates the mechanical behaviors of SPR joints at three test speeds. The static strength and stiffness are higher than the dynamic values, while the toughness is lower, which could also be the result of differences in the strain rate effect between substrate

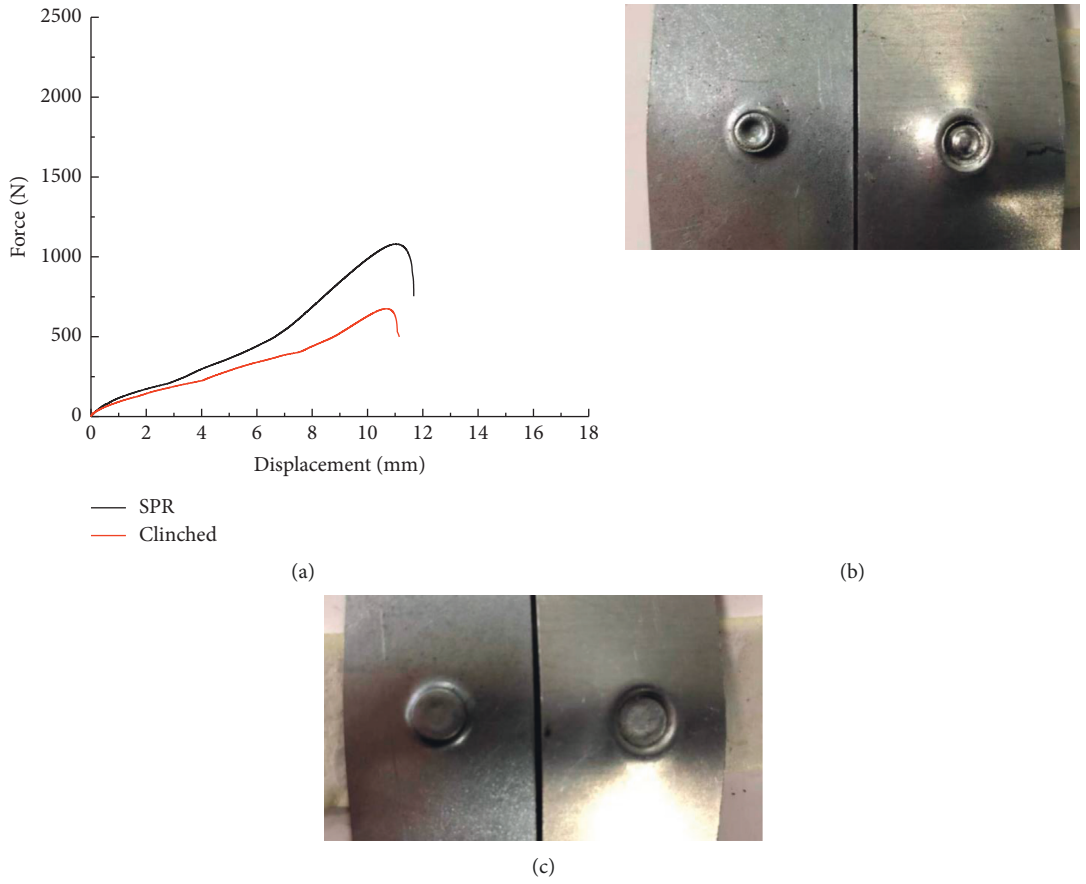

Figure 4: Static cross-tension tests: (a) force-displacement curves, (b) pulling-out failure modes of SPR joint, and (c) clinched joint at 0.083×10^{-3} m/s.

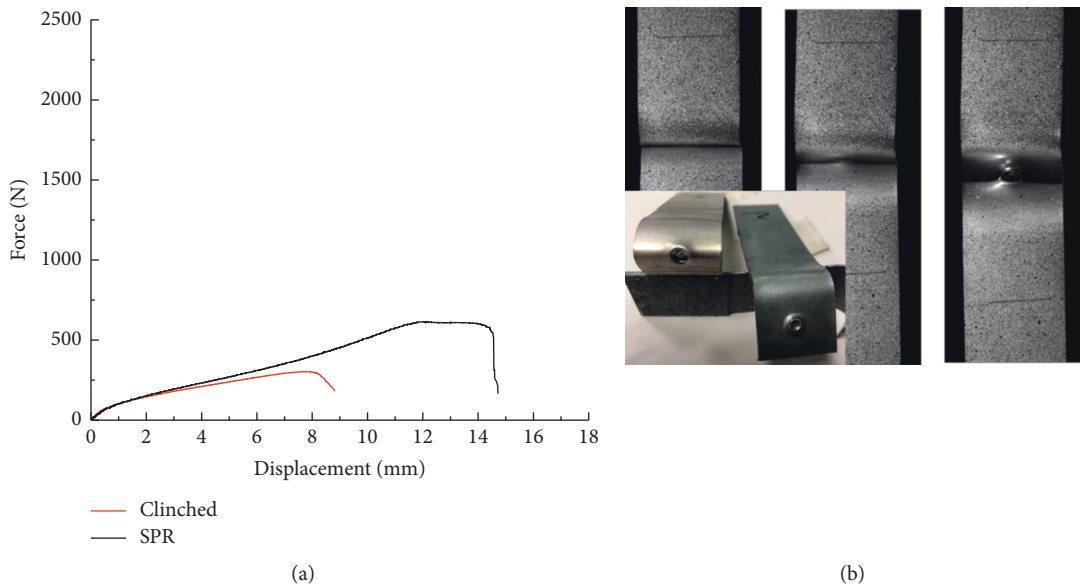

Figure 5: Continued.

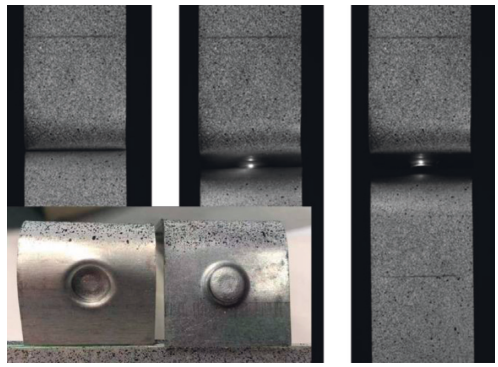

(c)

Figure 5: Static coach-peel tests: (a) force-displacement curves, (b) deformation process of SPR joint, and (c) clinched joint at 0.083×10^{-3} m/s.

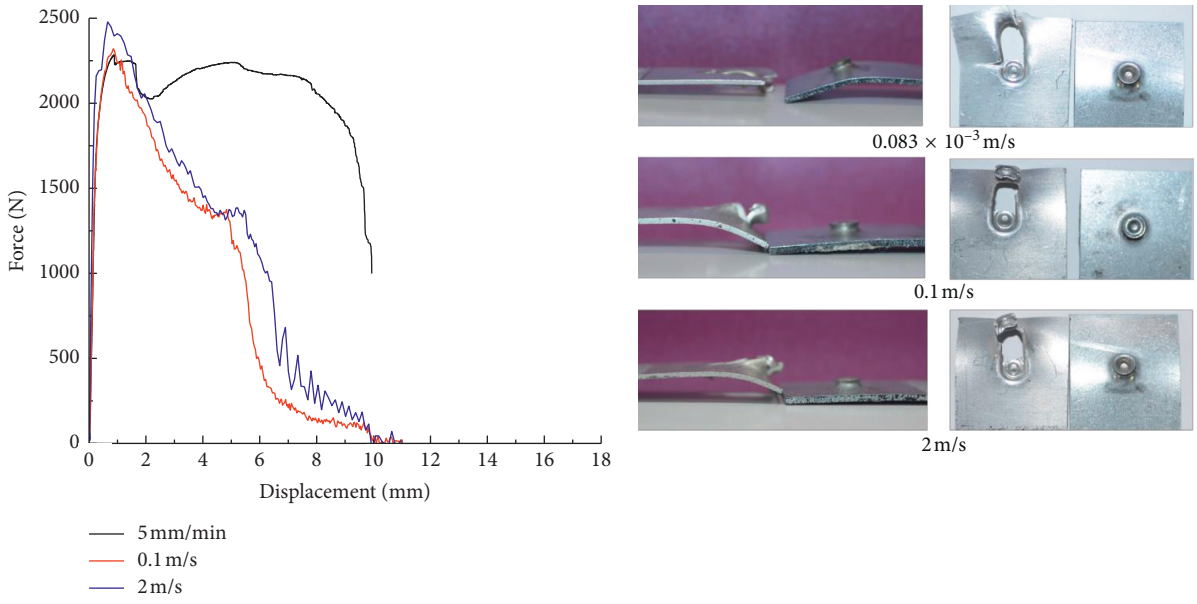

(a) (b)

Figure 6: Dynamic lap-shear tests of SPR joints: (a) force-displacement curves and (b) failure modes at three speeds.

materials. As the yielding stress increases, the deformation of the steel sheet is delayed, so that the stiffness of the specimen is more dependent on the bending stiffness of the aluminum sheet, which decreases. The failure modes at the three speeds are all unbuttoning without material fracture on either steel or aluminum sheets. The static energy absorption is approximately 5.5 J, and the dynamic absorption is approximately 5.4 J, which indicates that although the mechanical behavior is influenced by the loading speed for coach-peel specimens, the energy absorption capability is not.

The dynamic response of a clinched joint to shear loading is different from that of an SPR joint. As shown in Figure 8, although the stiffness is not sensitive to the loading speed, the maximum strength and ductility increase with the loading speed. The distortion of interlocks leads to unbuttoning and pull-out failure mode of the joints at all three speeds. The deformation pattern of the steel and aluminum sheets is also similar; that is, the steel sheet is bent, and the aluminum sheet remains flat. However, the local doming on the aluminum sheet is enlarged. This helps prevent the button from being pulled out. It could be a result of the earlier deformation of aluminum under dynamic conditions. It is noteworthy that although the strength and ductility are enhanced by the dynamic effect, the energy absorption of clinched joints exposed to lap-shear condition is much less than that of the SPR joints, which are approximately 2.2 J for the static condition, 3.5 J for 0.1 m/s, and 5 J for 2 m/s.

Correspondingly, the clinched joint under coach-peel condition is enhanced by the loading speed. Both the maximum strength and ductile are enlarged. The total energy absorption capability increases from 1.8 (5 mm/min) to 1.9 J under 0.1 m/s and 2.2 J under 2 m/s, as shown in Figure 9. Although the mechanical responses are different, the deformation patterns under three speeds are quite the

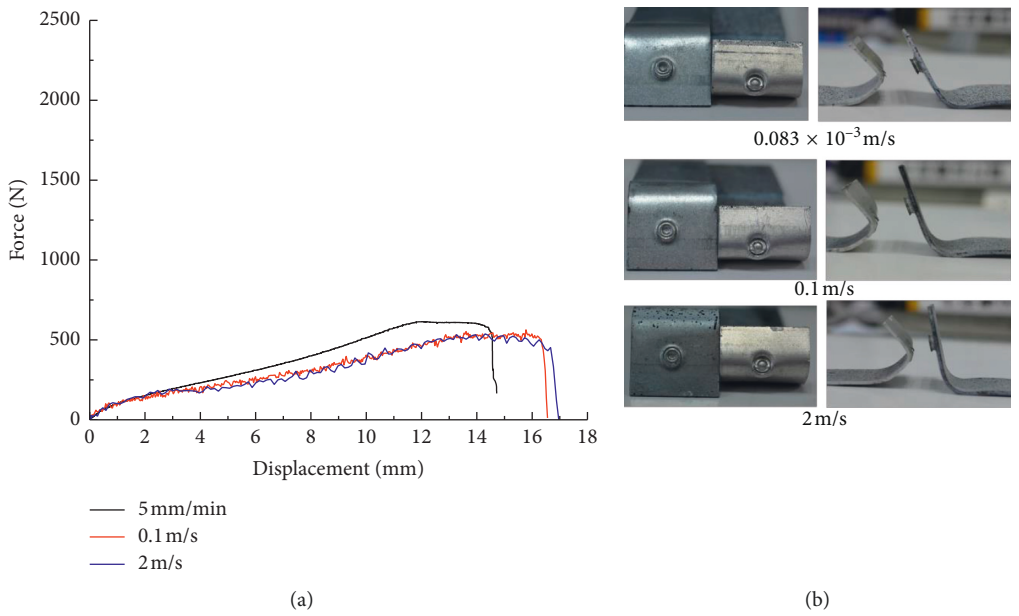

Figure 7: Dynamic coach-peel tests of SPR joints: (a) force-displacement curves and (b) failure modes at three speeds.

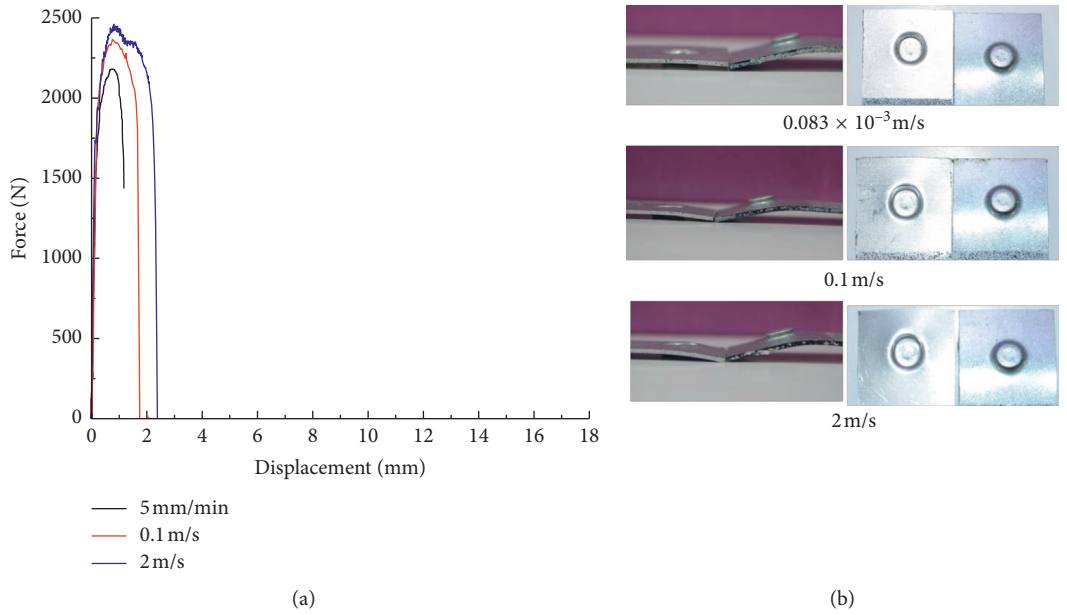

Figure 8: Dynamic lap-shear tests of clinched joints: (a) force-displacement curves and (b) failure modes at three speeds.

same. The steel sheet deforms little and the aluminum sheet is bent which results in the unbuttoning and pull-out failure. The curvature and distortion of the button is much less than the SPR ones. It implies that the significant dynamic effect of clinched joints under coach-peel condition could be the result of dynamic friction between the sheets.

To conclude, both joints of DX51 and AA5182-O combination under shear and normal load conditions have dynamic effects. However, the dynamic effects perform quite conflicting. The SPR joint tends to be weakened and the clinched joint tends to be strengthened by the effect due to the different strain rate effects of substrate materials and dynamic interface contacts.

4. Results of Baked Joint Tests

AA5182-O attains its strength through work hardening and exhibits softening during the paint bake cycle, which is very likely to occur for BIW, as shown in Figure 10. Because large plastic deformation occurs in both SPR and clinching joining processes, it can lead to mechanical modification in the present material combination.

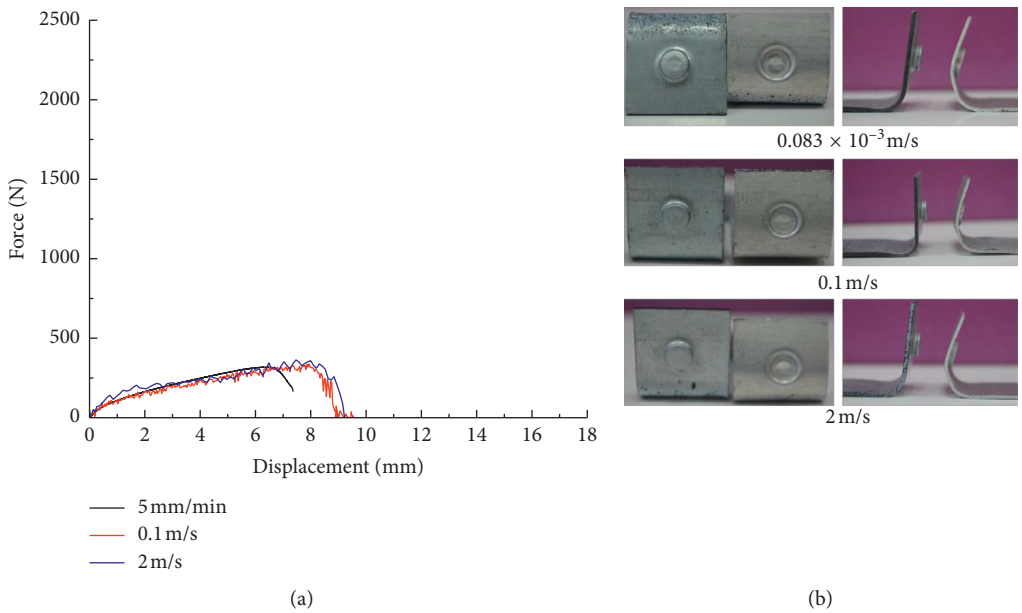

Figure 9: Dynamic coach-peel tests of clinched joints: (a) force-displacement curves and (b) failure modes at three speeds.

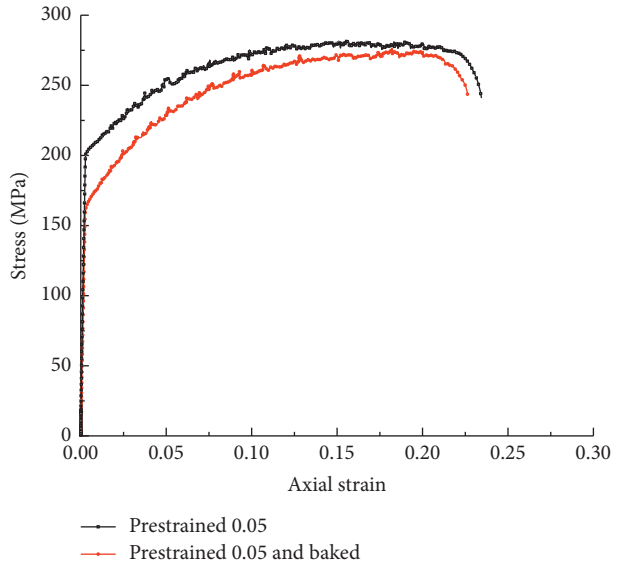

Figure 10: Quasistatic stress-strain curves of baked AA5182-O at 0.05 plastic deformation.

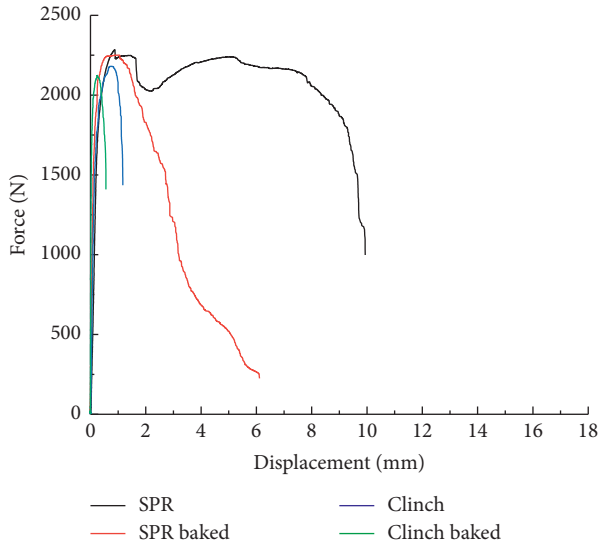

Figure 11: Comparison of lap-shear tests of SPR and clinched joints before and after the baking process at 0.083×10^{-3} m/s.

Figure 11 illustrates the force-displacement curves of lap-shear tests of SPR and clinched joints before and after the baking process. Both SPR and clinched joints have a higher stiffness and similar strength. Meanwhile, the ductility of the joints significantly decreases after baking, by up to 60%.

The cross-tension tests results demonstrate very different baking effect on the joints, as shown in Figure 12. The stiffness, strength, and ductility of all joints are quite similar. The joints' mechanical behavior in the normal direction is not sensitive to the baking softening of the AA5182-O bottom sheets.

In terms of coach-peel tests, completely converse responses to the baking process appear, compared with the lap-shear tests, as shown in Figure 13. The stiffness and maximum strength decrease after baking. The ductility, however, is less influenced by baking.

The test results indicate that both SPR and clinched joints of AA5182-O and DX51 suffer from the baking process. The baking effect, however, is loading condition-dependent and affects the specimens differently. Table 2 demonstrates the summary of the test results.

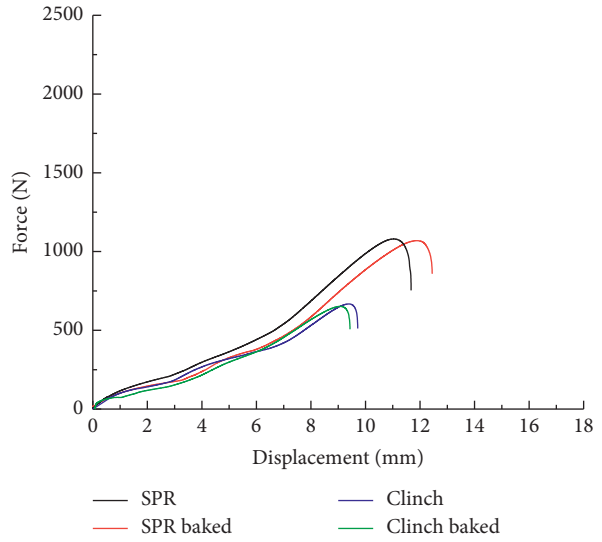

Figure 12: Comparison of cross-tension tests of SPR and clinched joints before and after the baking process at 0.083×10^{-3} m/s.

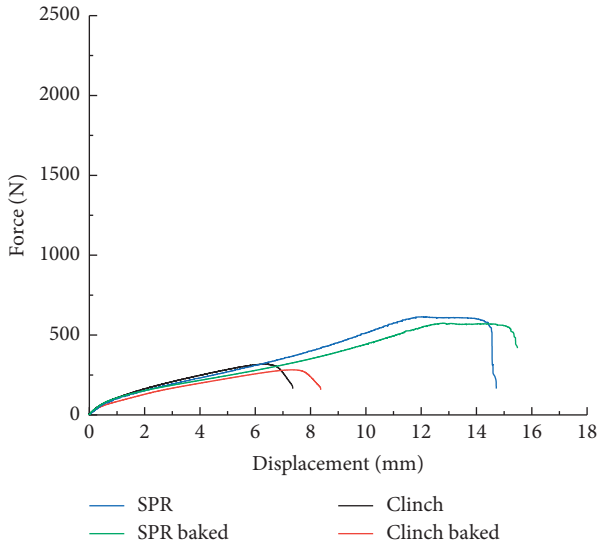

Figure 13: Comparison of coach-peel tests of SPR and clinched joints before and after the baking process at 0.083×10^{-3} m/s.

Table 2: Test result summary (units: speed m/s, force (N), and energy (J)).

Test speed	SPR		SPR baked		Clinch		Clinch baked	
	Peak force	Total energy absorption	Peak force	Total energy absorption	Peak force	Total energy absorption	Peak force	Total energy absorption
				Lap-shear				
0.083×10^{-3}	2280	21.0	2251	7.7	2180	2.1	2123	1.5
0.1	2320	10.1	—	—	2366	3.5	—	—
2	2477	11.9	—	—	2461	5.1	—	—
				Coach-peel				
0.083×10^{-3}	614	5.5	574	5.4	302	1.8	282	1.6
0.1	536	5.4	—	—	322	1.9	—	—
2	524	5.4	—	—	350	2.2	—	—
				Cross-tension				
0.083×10^{-3} m	1180	5.9	1069	6.1	675	3.1	652	2.9

5. Conclusions

Experiments on SPR and mechanical clinched joints of AA5182-O and DX51 with various loading directions, speeds, and heat treatments were realized. The energy absorption of SPR joints is much higher under all conditions. The dynamic and baking effects on the mechanical behaviors of these two joining methods were compared.

(i) The failure modes of SPR joints of dissimilar materials are direction-sensitive. Substrate material failure on aluminum is the primary mode under lap-shear conditions, and tail pulling-out dominates the cross-tension and coach-peel conditions. Clinched joints commonly fail by pulling-out, where the steel sheet separates from the bottom sheet.

(ii) Dynamic effects on joints of dissimilar materials are loading condition-dependent. The strength of the two joints under lap-shear conditions increases with increasing loading rate. However, the dissipated energy of the SPR joint decreases because of the loss of load-bearing capability of the rivet tail, and that of the clinched joint increases. Under the coach-peel condition, the strength of the SPR joint decreases with increasing loading rate and the dissipated energy stays the same. However, both strength and the total energy absorption capability of the clinched joint increase under dynamic conditions.

(iii) The baking process significantly affects the mechanical behavior of SPR and clinched joints and is loading direction-dependent. Both joints are weakened under lap-shear and coach-peel conditions, but the baking process has a negligible influence under cross-tension conditions.

Data Availability

The experimental data used to support the findings of this study are included within the article.

Conflicts of Interest

The authors declare that there are no conflicts of interest regarding the publication of this paper.

Acknowledgments

This was sponsored by the Key D&R Program of China under contract no. 2016YFB0101606. The author would like to acknowledge the staff at Suzhou Automotive Research Institute of Tsinghua University (TSARI) for providing technical support in conducting experiments.

References

[1] X. He, I. Pearson, and K. Young, "Self-pierce riveting for sheet materials: state of the art," *Journal of Materials Processing Technology*, vol. 199, no. 1–3, pp. 27–36, 2008.

[2] K. Martinsen, S. J. Hu, and B. E. Carlson, "Joining of dissimilar materials," *CIRP Annals—Manufacturing Technology*, vol. 64, no. 2, pp. 679–699, 2015.

[3] D. Li, A. Chrysanthou, I. Patel, and G. Williams, "Self-piercing riveting-a review," *The International Journal of Advanced Manufacturing Technology*, vol. 92, no. 5–8, pp. 1777–1824, 2017.

[4] R. Haque, Y. C. Wong, A. Paradowska, S. Blacket, and Y. Durandet, "SPR characteristics curve and distribution of residual stress in self-piercing riveted joints of steel sheets," *Advances in Materials Science and Engineering*, vol. 2017, Article ID 5824171, 14 pages, 2017.

[5] L. Kaðèák, E. Spiðák, R. Kubík, and J. Mucha, "Finite element calculation of clinching with rigid die of three steel sheets," *Strength of Materials*, vol. 49, no. 4, pp. 488–499, 2017.

[6] G. Meschut, V. Janzen, and T. Olfermann, "Innovative and highly productive joining technologies for multi-material lightweight car body structures," *Journal of Materials Engineering and Performance*, vol. 23, no. 5, pp. 1515–1523, 2014.

[7] J. Mucha, "The analysis of lock forming mechanism in the clinching joint," *Materials & Design*, vol. 32, no. 10, pp. 4943–4954, 2011.

[8] J. Mucha and W. Witkowski, "The clinching joints strength analysis in the aspects of changes in the forming technology and load conditions," *Thin-Walled Structures*, vol. 82, pp. 55–66, 2014.

[9] J. Mucha, L' Kaščák, and E. Spišák, "The experimental analysis of cold pressed joint technology for selected sheet metals used in an automotive industry," *Advanced Materials Research*, vol. 1077, pp. 33–38, 2014.

[10] J. P. Varis, "The suitability of clinching as a joining method for high-strength structural steel," *Journal of Materials Processing Technology*, vol. 132, no. 1–3, pp. 242–249, 2003.

[11] K. Mori, Y. Abe, and T. Kato, "Mechanism of superiority of fatigue strength for aluminium alloy sheets joined by mechanical clinching and self-pierce riveting," *Journal of Materials Processing Technology*, vol. 212, no. 9, pp. 1900–1905, 2012.

[12] B. Xing, X. He, Y. Wang, H. Yang, and C. Deng, "Study of mechanical properties for copper alloy H62 sheets joined by self-piercing riveting and clinching," *Journal of Materials Processing Technology*, vol. 216, pp. 28–36, 2015.

[13] R. Haque and Y. Durandet, "Strength prediction of self-pierce riveted joint in cross-tension and lap-shear," *Materials & Design*, vol. 108, pp. 666–678, 2016.

[14] X. Sun and M. A. Khaleel, "Dynamic strength evaluations for self-piercing rivets and resistance spot welds joining similar and dissimilar metals," *International Journal of Impact Engineering*, vol. 34, no. 10, pp. 1668–1682, 2007.

[15] R. Porcaro, M. Langseth, A. G. Hanssen, H. Zhao, S. Weyer, and H. Hooputra, "Crashworthiness of self-piercing riveted connections," *International Journal of Impact Engineering*, vol. 35, no. 11, pp. 1251–1266, 2008.

[16] A. Chrysanthou and X. Sun, *Self-piercing Riveting: Properties, Processes and Applications*, Woodhead Publishing, Sawston, UK, 2014.

[17] Z. Gronostajski and S. Polak, "The application of clinching techniques to join impact energy absorbing thin-walled aluminium sections," *Archives of Metallurgy and Materials*, vol. 54, no. 3, pp. 695–703, 2009.

[18] G. B. Burger, A. K. Gupta, P. W. Jeffrey, and D. J. Lloyd, "Microstructural control of aluminum sheet used in automotive applications," *Materials Characterization*, vol. 35, no. 1, pp. 23–39, 1995.

[19] H. Yamada, T. Kami, R. Mori, T. Kudo, and M. Okada, "Strain rate dependence of material strength in AA5xxx series aluminum alloys and evaluation of their constitutive equation," *Metals*, vol. 8, no. 8, pp. 576–591, 2018.

[20] N. Weiß-Borkowski, J. Lian, T. Marten, T. Tröster, S. Münstermann, and W. Bleck, "Forming limit curves determined in high-speed Nakajima tests and predicted by a strain rate sensitive model," in *AIP Conference Proceedings*, vol. 1896, Dublin, Ireland, October 2017.